Adverse pulmonary effects after oral exposure to copper, manganese and mercury, alone and in mixtures, in a Spraque-Dawley rat model

[1]Draper M, [1]Bester MJ, [2]Van Rooy M, [1]Oberholzer HM

[1]Department of Anatomy, Faculty of Health Sciences, University of Pretoria, Private Bag x323, Arcadia, 0007, South Africa

[2]Department of Physiology, Faculty of Health Sciences, University of Pretoria, Private Bag x323, Arcadia, 0007, South Africa

*** Address correspondence to** H.M. Oberholzer, Department of Anatomy, Faculty of Health Sciences, University of Pretoria Private Bag x323, Arcadia 0007, South Africa.

Phone: 012 319 2533, E-mail: nanette.oberholzer@up.ac.za.

Abstract

The rise in respiratory disease has been attributed to an increase in environmental pollution. Heavy metals contribute to environmental contamination via air, water, soil and food. The effects of atmospheric exposure to heavy metals on pulmonary structure and function have been researched, but the effects through drinking water have been neglected. The aim of this study was to investigate the potential *in vivo* alterations in the pulmonary tissue of male Sprague-Dawley rats after a 28-day oral exposure to copper (Cu), manganese (Mn) and mercury (Hg), alone and in mixtures, at 100 times the World Health Organisation's (WHO) safety limit for each heavy metal in drinking water. Forty-eight male Sprague-Dawley rats were randomly divided into eight groups (n=6): control, Cu, Mn, Hg, Cu + Mn, Cu + Hg, Mn + Hg and Cu, Mn + Hg. The morphology of lung tissue and the bronchioles were evaluated using light- and transmission electron microscopy. For all exposed groups, morphological changes included thickened inter- and intra-alveolar spaces, stratified epithelium, disrupted smooth muscle and early fibrosis and desquamation of the epithelia of the bronchioles to varying degrees. In all exposed groups, ultrastructurally, an increase in disarranged collagen and elastin fibres, nuclear membrane detachment, chromatin condensation, indistinct nucleoli and an increase in collagen fibre disarrangement was observed. This study has identified that oral exposure to Cu, Mn and Hg and as part of mixtures caused pathogenesis due to inflammation, cellular damage and fibrosis with Mn + Hg being the most potent heavy metal group.

Keywords: Heavy metals, copper, manganese, mercury, metal mixture, bronchiole, toxicity

Introduction

The pulmonary system, due to its function, is constantly exposed to airborne agents.[1] However, the respiratory system is vulnerable to both inhaled and ingested environmental pollutants.[2] For decades, Africa has been impacted by respiratory communicable diseases, such as tuberculosis. More recently the incidence of non-communicable respiratory diseases is on the rise due to smoking and the inhalation of environmental pollutants.[3,4] These diseases include both acute and chronic respiratory diseases, such as acute respiratory distress syndrome (ARDS), chronic obstructive pulmonary disease (COPD), asthma, idiopathic pulmonary fibrosis (IPF) and cancer.[1]

Acute respiratory distress syndrome is an alveolar pathology, caused by an increase in hydrostatic pressure in the alveolar capillaries or damage to the epithelial lining of alveoli or damage to the endothelial lining of the alveolar capillaries. The damage or increase in pressure causes fluid leakage from the alveolar capillaries into the interstitium and alveolar spaces.[5] Asthma is the most common chronic childhood disease characterized by airway hyper-responsiveness, cytokine-induced inflammation, and airway obstruction and remodelling resulting in an increase in sub-epithelial and epithelial thickness and an increase in the number of macrophages, eosinophils, basophils, goblet and mast cells. [6,7] Histological pathologies of asthmatic individuals include epithelial detachment, hypertrophy of smooth muscle, sub-epithelial thickening, collagen deposition and infiltration of inflammatory cells. [8]

Chronic obstructive pulmonary disease is a major global health burden with no cure and is considered a combination of chronic bronchitis and emphysema. [9] It is characterised by airflow restriction, leading to increased resistance to airflow, due to an abnormal inflammatory response to stimuli, such as noxious gases. [9] Pathological changes of COPD include hyper-production and secretion of mucus associated with chronic bronchitis, obstructive bronchiolitis

due to remodelling of small airways, pulmonary vessel wall thickening, emphysematous destruction, and hyperinflation. [9] As resistance to airflow increases this results in decreased expiratory volumes where individuals suffering from COPD struggle to exhale air. [9] A greater degree of inflation is consequently required to increase the pressure gradient between the alveolar- and atmospheric pressure allowing air to be expired. [9] Emphysema is the dilation of terminal bronchioles and alveoli due to oxidative damage, tissue remodelling and fibrosis of alveolar walls by environmental irritants and pollutants. [10-13] An increase in inflammatory cells, erythrocytes within the alveolar capillaries and re-arranged collagen fibres are histopathological features.[11] Idiopathic pulmonary fibrosis is a chronic interstitial pulmonary disease that occurs due to alveolar inflammation that results in epithelial damage, repair, and remodelling of the pulmonary tissue with progression to fibrosis. [14-16] Histopathological examination of pulmonary fibrosis has shown an increase in inflammatory cells and subsequent increase in extra-cellular matrix (ECM) – such as collagen, alveolar thickening, increase in type II pneumocytes and desquamation/cuboidalisation of epithelium. [14, 17,18] Fibrosis will decrease lung compliance making it more difficult for the lungs to expand and decreasing the volume of air that can be inspired and that can be used for gas exchange.[19]

These pathologies are all associated with oxidative stress and an increase resistance of pulmonary flow that will adversely affect gas exchange and ultimately blood oxygen levels. [1,20] Aetiological risk factors include the exposure to environmental pollutants such as heavy metals from smoking and cooking with solid fuels.[4] Usually, heavy metals are generally found as mixtures of two or more metals, and are often associated with other compounds at varying concentrations and cannot be destroyed or degraded and over time can bio-accumulate.[21] The adverse health effects due to the exposure to toxicants is increasing globally, and the effects of heavy metals are long lasting.[22] Inhalation of heavy metals, copper (Cu), manganese (Mn) and

mercury (Hg) are all associated with pulmonary inflammation, which can result in airway obstruction and pulmonary embolism that is often fatal. [23-25]

Ultrastructural changes to organelles, associated with heavy metals, can also compromise cellular functioning in tissues and organs. Cell injury occurs when homeostasis is disrupted at the molecular level. Many factors can cause cell injury, but the basic mechanisms include: adenosine triphosphate (ATP) depletion, cell membrane damage, disturbance to any biochemical pathway and deoxyribonucleic acid (DNA) damage, in isolation or in combination.[26] Specifically mitochondrial and membrane damage, that is associated with cellular necrosis and the ageing process, is mediated by reactive oxygen species (ROS). [26]

The aim of this study was to investigate the effects of Cu, Mn and Hg exposure via oral gavage, alone and in mixtures, on the morphology and ultrastructure of the pulmonary tissue of Sprague-Dawley (SD) rats following gavage-dosing for 28 days.

Materials and methods

Metal preparation

This study used male SD rats exposed to either saline only (control) or to Cu, Mn and Hg, alone and in mixtures. Administration of the aqueous solutions of copper (II) sulphate ($CuSO_4.5H_2O$, purity: 98%), manganese (II) chloride ($MnCl_2.4H_2O$, purity: 99%), mercuric chloride powder ($HgCl_2$, purity: 99%) and 0.9% sodium chloride (NaCl, purity: 99%), which were dissolved in distilled, deionised water (ddH_20), administered via oral gavage. All metal salts were purchased from Sigma-Aldrich, Johannesburg, South Africa. All other reagents were obtained from Sigma Aldrich, Johannesburg, South Africa unless otherwise specified.

Dosage calculations

The final concentration of the daily dosage solutions for each metal and the mixtures are presented in Table 1. The selected concentrations were based on and were X100 greater than the 2011 World Health Organisation's (WHO) drinking water guideline values, for each respective metal.[27] The dosage concentration was chosen based on previous studies that demonstrated moderate adverse effects at the X100 and X1000 WHO concentrations on various systems, including the cardiovascular system (heart and aorta), respiratory system and blood components, exposed to different heavy metal combinations 3, 28-30.

Table 1: Daily dosage calculations for the oral gavage solutions of the experimental groups.

	Cu	**Mn**	**Hg**
WHO limit (mg/L)	**2.0**	**0.4**	**0.006**
WHO limit X 100 (mg/L)	200.0	40.0	0.6
Molecular weight: metal (g/mol)	63.5	54.9	200.6
Metal ion concentration (mM)	3.147	0.728	0.003
Molecular weight: metal-salt (g/mol)	249.7	197.9	271.5
Metal salt concentration (g/L)	0.786	0.144	0,0008
Daily intake (g/2L)	1.572	0.288	0.0016
Human (60 kg) daily intake (mg/kg)	26.2	4.8	0.027
Rat (150 g) intake (mg/kg)	161.5	29.6	0.17
Dosage solutions (mg/mL)	**48.5**	**8.9**	**0.05**

*Note: Mixtures contain the same (mg) of each respective metal.

The calculated concentrations were based on a 60 kg adult drinking 2 L of water a day. A 150 g rat equivalent dosage was then calculated, using the following equation:

Rat equivalent dose (mg/kg) = Human equivalent dose (mg/kg) / dosage factor*

*Dosage factor being rat Km/human Km, with the human Km = 37 and the rat Km = 6.

The dosage factor for conversion from rat to human is 6/37. Km is a correction factor used based off the surface area of a species. [31] Therefore, the rat equivalent dose was 161.5, 29.6 and 0.17 mg/kg/day for Cu, Mn and Hg, respectively.

Sprague-Dawley rat model

Six-week-old male SD rats (150 g) were obtained from the Onderstepoort Veterinary Animal Research Unit (OVARU). Standard irradiated "Epol" rat pellets and municipal water were provided *ad libitum.* The animals were housed in conventional cages complying with the sizes described in the South African National Standards (SANS) 10386:2008 recommendations. A room temperature of 22°C (±2°C); relative humidity of 50% (±20%) and a 12-hour light/dark cycle was maintained during the entire study. The rats were housed in pairs in cages with autoclaved pinewood shavings as bedding material. White facial tissue paper was added for enrichment according to standard procedures at the University of Pretoria Biomedical Research Centre (UPBRC). The rats were acclimatized for 7 days prior to the start of the 28-day experimentation period. Ethical approval was obtained from the University of Pretoria's Animal Ethics Committee (AEC) with approval number 6/2019.

Forty-eight male rats were included and were randomly divided into eight groups (six rats per group), as follows: control, Cu, Mn, Hg, Cu + Mn, Cu + Hg, Mn + Hg and Cu, Mn + Hg (The control group received a saline solution, 0.9% NaCl, only). The seven experimental groups received the metal mixtures assigned, at a X100 the WHO safety limit for drinking water (2mg/L for Cu, 0.4mg/L for Mn and 0.06 mg/L for Hg). [27] A rat equivalent dosage was then calculated.[31] All rats were administered 0.5 mL of the respective solutions daily through oral

gavage, for 28 days. The rats were weighed bi-weekly to identify any sudden change in weight and the behaviour of the rats was monitored daily. The rats were terminated on day 28 via isoflurane (general anaesthesia) overdose and cardiac puncture, according to the standard methods employed by the UPBRC. Organs were harvested on the day of termination after blood collection via dissection. Pulmonary tissue was harvested for morphological and ultrastructural analyses.

Light microscopy sample preparation

Following termination, the pulmonary tissue was dissected from each animal and processed for light microscopy as described by Naidoo *et al*., 2019. The tissue samples were fixed in 4% formaldehyde (FA) in 0.1 M phosphate buffer solution (PBS) [0.2 M disodium phosphate (Na_2HPO_4), 0.2 M sodium dihydrogen phosphate monohydrate ($NaH_2PO_4 \cdot H_2O$), 0.15 M sodium chloride (NaCl), pH: 7.4]. The samples were then washed three times for 30 minutes with 0.1 M PBS, before dehydration using increasing serial concentrations of 50% ethanol (EtOH) (Merck, Johannesburg, South Africa) for 30 minutes, 70% EtOH for one hour, 90% EtOH for one hour, twice in 100% EtOH for one hour and left overnight in 100% EtOH. The samples were infiltrated with paraffin wax by first placing the samples in a 1:1 xylene and EtOH mixture for 30 minutes, then 100% xylene for 2 hours, followed by 3:7 wax in xylene mixture for one hour, 7:3 wax in xylene mixture for one hour and finally in 100% wax for two hours, all steps at 60˚C. The samples were embedded in paraffin wax, cooled to 4˚C and then sections of 5 µm were prepared with a Leica RM 2255 wax microtome (Leica Microsystems, Wetzlar, Germany) and placed on glass slides. The sections were de-waxed by placing the slides twice in 100% xylene for five minutes, and then twice in 100% EtOH for two minutes followed by rehydration in 90% and 70% EtOH for one minute each and finally in ddH_2O for

1 minute.[3] The slides were then stained with Haematoxylin and Eosin (H&E) and Picrosirius red (PR) to evaluate general morphology and collagen distribution (fibrosis), respectively

Haematoxylin and eosin staining

To evaluate alveolar and bronchiole morphology H&E staining was performed as previously described by Naidoo *et al*., 2019.[3] A 0.1% haematoxylin stain solution was prepared by dissolving 1 g of haematoxylin in 1 L of ddH_2O. To this 0.2 g of sodium iodate and 50 g of potassium aluminium sulphate were then added and dissolved before adding 1 g citric acid and 50 g chloral hydrate. To prepare the eosin stain, 2 g of yellowish eosin powder was dissolved in 200 mL of ddH_2O. Scott‘s buffer solution was made by dissolving 2 g of potassium bicarbonate and 20 g of magnesium sulphate in 1 L ddH_2O. The sectioned slides were cleared with xylene for 10 min and were rehydrated in a series of decreasing concentrations of EtOH; two changes of 100% EtOH, 90% and 70% each for 1 min. The slides were then placed in ddH_2O for 1 min, haematoxylin for 15 min and Scott's buffer for 8 min. The slides were then rinsed with ddH_2O and then dipped in eosin to counterstain, ascending series of EtOH for rehydration (70% EtOH, 90% EtOH, 100% EtOH) and xylene before the coverslips were mounted with Entellan® mounting medium.[3] The slides were viewed with a Zeiss AXIO Imager.M2 (Zeiss, Oberkochen, Germany) light microscope. Representative images of each group were used to evaluate the changes in tissue general morphology.

Picrosirius red staining

The PR staining and polarisation method was used to evaluate the orientation of collagen fibres in different tissues under different pathological and physiological states (Latouff *et al*., 2014).[32] Collagen appears red, green or yellow under polarized light. A strong yellow-red birefringence indicates collagen type I and a weak greenish birefringence indicates collagen

type III.[32] The dye solution was prepared by dissolving 0.5 g of Sirius Red dye in 500 mL of a saturated aqueous solution of picric acid. Acidified water was used for washing, prepared by adding 5 mL of glacial acetic acid to 1 L of ddH_2O. The tissue was first stained in haematoxylin for eight minutes and then rinsed under running tap water for ten minutes. The PR solution was applied for 1 hr and the slides were washed twice with acidified water before dehydration three times in 100% EtOH and cleared with xylene before the coverslip was mounted using Entellan.[33] The slides were viewed with a Zeiss AXIO Imager.M2 (Zeiss, Oberkochen, Germany) light microscope, under brightfield and polarizing light. Representative images of each group were used to evaluate the changes in tissue collagen distribution (fibrosis).

Transmission electron microscopy sample preparation

For ultrastructural studies of pulmonary tissue, transmission electron microscopy (TEM) was performed. Samples were obtained from the same area as for light microscopy. The tissue was cut into small pieces of approximately 1 mm^3 in size and then was fixed in a 2.5% glutaraldehyde/formaldehyde (GA/FA) (Sigma-Aldrich, Johannesburg, South Africa) (5 mL 0.075 M PBS – pH 7.4), 1 mL GA, 1 mL FA and 3 mL ddH_2O solution for one hr before being washed three times for 15 minutes in PBS. This was followed by secondary fixation in 1% osmium tetroxide (Sigma-Aldrich, Johannesburg, South Africa) for one hr and washed as described above. The samples were dehydrated by using an increasing serial dehydration step with 30%, 50%, 70% and 90%, followed by three changes of 100% EtOH, 15 minutes for each step. The samples were then left overnight in 100% EtOH and then were finally embedded in resin (Arbi *et al*., 2021). The resin blocks were trimmed and ultra-thin sections (100 nm) were prepared with an ultramicrotome. Samples were contrasted with uranyl acetate for three minutes followed by three minutes of contrasting with lead citrate, after which samples were allowed to air dry before being examined with the JEOL JEM 2100F transmission electron

microscope (JEOL Ltd., Tokyo, Japan). Representative images of each group were used to evaluate the changes in tissue ultrastructure.

Tissue evaluation

This observational qualitative study of eight animal groups, consisting of the control and seven heavy metal exposed groups, aimed to describe the general structure (H&E staining) and fibrosis (PR staining) in the pulmonary tissue using light microscopy (LM) and the ultrastructure using TEM. The changes in tissue structure in the exposed groups were compared with the control group. Six rats were included in each group and for each staining method two slides from each rat were analysed with LM and for each of the tissues two grids for each animal were analysed with TEM.

For comparative purposes a scoring system was used, where the degree of change was evaluated. The parameters that were evaluated using LM in the pulmonary tissue were the extent of inter- and intra-alveolar thickening, changes in the area of the intra-alveolar space, presence of stratified epithelium, smooth muscle disruption and desquamation of the epithelium. The parameters that were evaluated using TEM in the pulmonary tissue were the extent of collagen and elastin fibre increase, heterochromatin condensation, indistinction of nucleolus and nuclear membrane detachment. For all the parameters the scoring was –: no or minimal alterations; +: slight alteration; ++: moderate alteration and +++: severe alteration based on the degree of change of the tissues.

Results

Haemotoxylin and eosin

The general histology of pulmonary tissue was evaluated with H&E and representative images, at X40 magnification, are shown in Figures 1 and 2. In Figure 1 A, the alveolar tissue of the control (saline) group has a well-defined alveolar space (A), thin epithelial walls, fine interstitium, type I (P1) and II (P2) pneumocytes and capillaries (c) containing erythrocytes (Er). The alveolar tissues of the experimental groups are presented in Figures 1 B - H. The histological architecture of the pulmonary tissue shows thickened inter-alveolar septa (red arrows) and altered intra-alveolar (green arrows) spaces in all the experimental groups (B to H). In Figure 2 A, the bronchiole structure of the control (saline) group is depicted and has an intact epithelial lining (E) and smooth muscle (SM) surrounding the bronchiole. The bronchiole tissue of the experimental groups are presented in Figures 2 B - H. Histological architecture of the bronchioles shows stratification of epithelium (SE), disrupted smooth muscle (black ring) and desquamation of the epithelia (asterisk) to varying degrees in all the experimental groups (B to H). Stratification of epithelia occurs due to the metaplasia of normal pseudostratified pulmonary epithelia to an abnormal stratified form.[34,35] The desquamation is evident by the presence of cellular debris within the bronchioles.

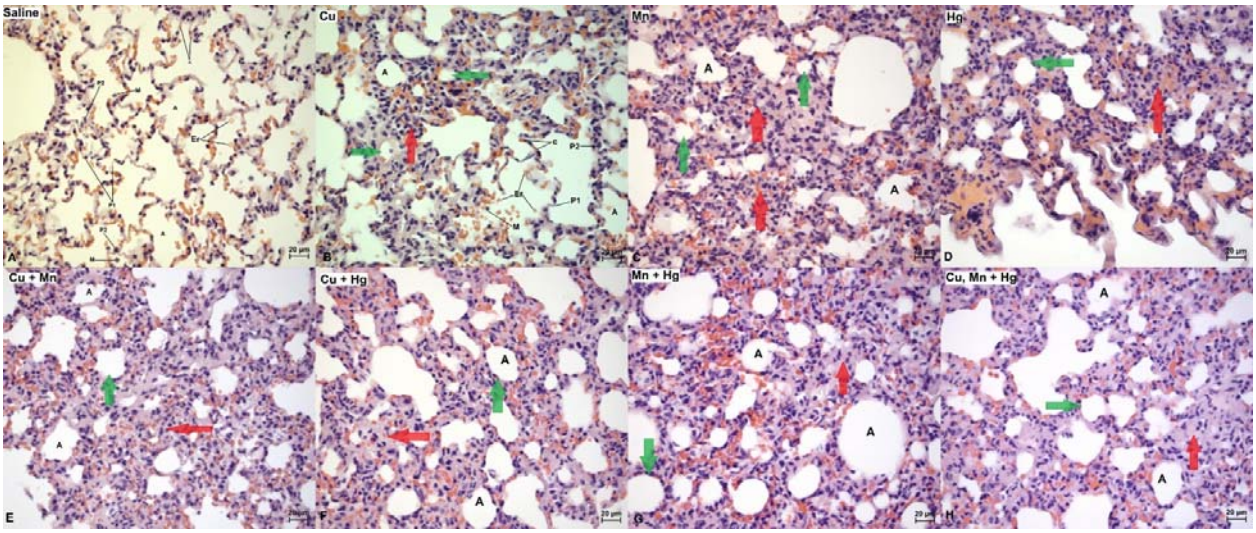

Figure 1: Photomicrographs of SD rat pulmonary tissue stained with H&E; Scale bar = 20 µm. **A**: Control, **B**: Cu, **C**: Mn, **D**: Hg, **E**: Cu + Mn, **F**: Cu + Hg, **G**: Mn + Hg, and **H**: Cu, Mn + Hg. **P1**: Type I pneumocyte; **P2**: Type II pneumocyte; **A**: Alveolar space; **Er**: Erythrocyte; **M**: Macrophage; **c**: Capillaries; **Red arrow**: Thickening of inter-alveolar septa and **Green arrow**: Intra-alveolar space area change

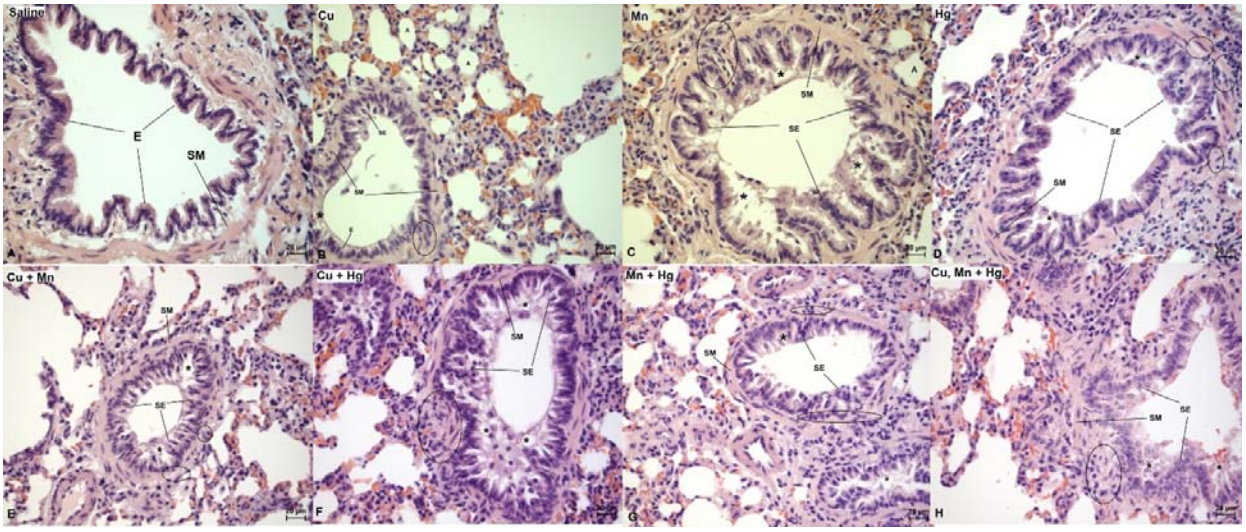

Figure 2: Photomicrographs of SD rat pulmonary bronchioles stained with H&E; Scale bar = 20 µm. **A**: Control, **B**: Cu, **C**: Mn, **D**: Hg, **E**: Cu + Mn, **F**: Cu + Hg, **G**: Mn + Hg, and **H**: Cu, Mn + Hg. **E**: Epithelium; **SE**: Stratified epithelium; **Asterisk**: Desquamated epithelium; **SM**: smooth muscle and **Black ring**: Disruption in smooth muscle.

A summary of the morphological findings of the pulmonary tissue is presented in Table 2.

Table 2: Summary of the histological changes to the H&E stained pulmonary following metal exposure.

	Thickened inter-alveolar septa	Area change of intra-alveolar space	Stratified epithelium	Smooth muscle disruption	Desquamation of epithelia
Cu	+	+	+	+	+
Mn	++	++	++	+	+++
Hg	++	++	+	+	+
Cu + Mn	++	++	++	+	++
Cu + Hg	++	++	+++	+	+++
Mn + Hg	++	++	+	+	+
Cu, Mn + Hg	++	++	++	+	++

–: no or minimal alterations; +: slight alteration; ++: moderate alteration; +++: severe alteration

Picrosirius Red

Collagen differentiation and distribution in the bronchioles were evaluated using PR staining. Representative images, at X40 magnification, acquired from stained pulmonary tissue are shown in Figures 3 and 4. In Figure 3 A2, a representative bronchiole of the control (saline) group is depicted and demonstrates a dim yellow-green birefringence under polarized light. The bronchioles of the experimental groups are demonstrated in Figures 3 B – D and 4 E – H. An increase in yellow-red birefringence is evident in Cu, Cu + Mn, Mn + Hg and the triple mixture group (Figure 3 B2 and Figure 4 E2, G2 and H2). The Cu (Figure 3 B2) and Cu, Mn + Hg (Figure 4 H2) groups has a slight increase, with Mn + Hg (Figure 4 G2) having a moderate increase and Cu + Hg (Figure 4 F2) having a severe increase in yellow-red birefringence. An increase in yellow-green birefringence was evident in all experimental groups with Mn, Hg, Cu + Mn, Cu + Hg and Mn + Hg (Figure 3 C2, D2 and Figure 4 E2, F2 and G2) with a slight

increase, Cu (Figure 3 B2) a moderate increase and the triple mixture group (Figure 4 H2) a severe increase.

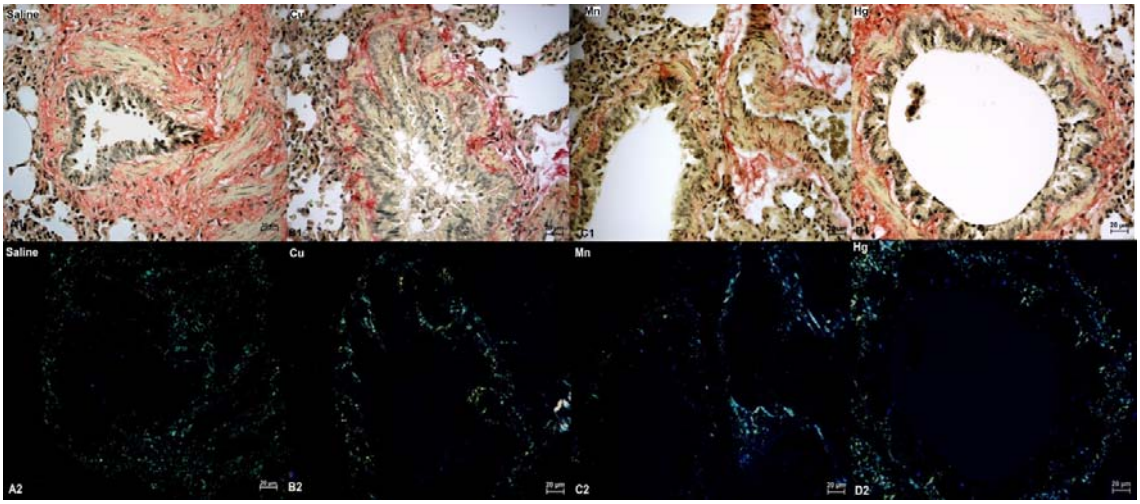

Figure 3: Photomicrographs of SD rat bronchioles stained with PR for the control and single heavy metal groups; Scale bar = 20 µm. **A**: Control, **B**: Cu, **C**: Mn, **D**: Hg, **E**: Cu + Mn, **F**: Cu + Hg, **G**: Mn + Hg, and **H**: Cu, Mn + Hg. **1**: Brightfield and **2**: Polarized light.

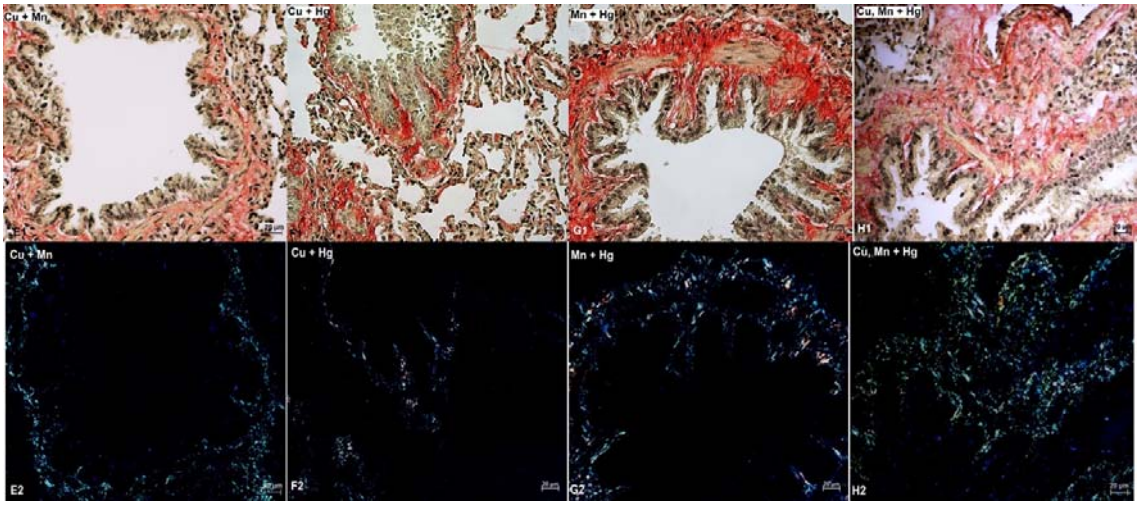

Figure 4: Photomicrographs of SD rat bronchioles stained with PR for the double and triple heavy metal mixture groups; Scale bar = 20 µm. **E**: Cu + Mn, **F**: Cu + Hg, **G**: Mn + Hg, and **H**: Cu, Mn + Hg. **1**: Brightfield and **2**: Polarized light.

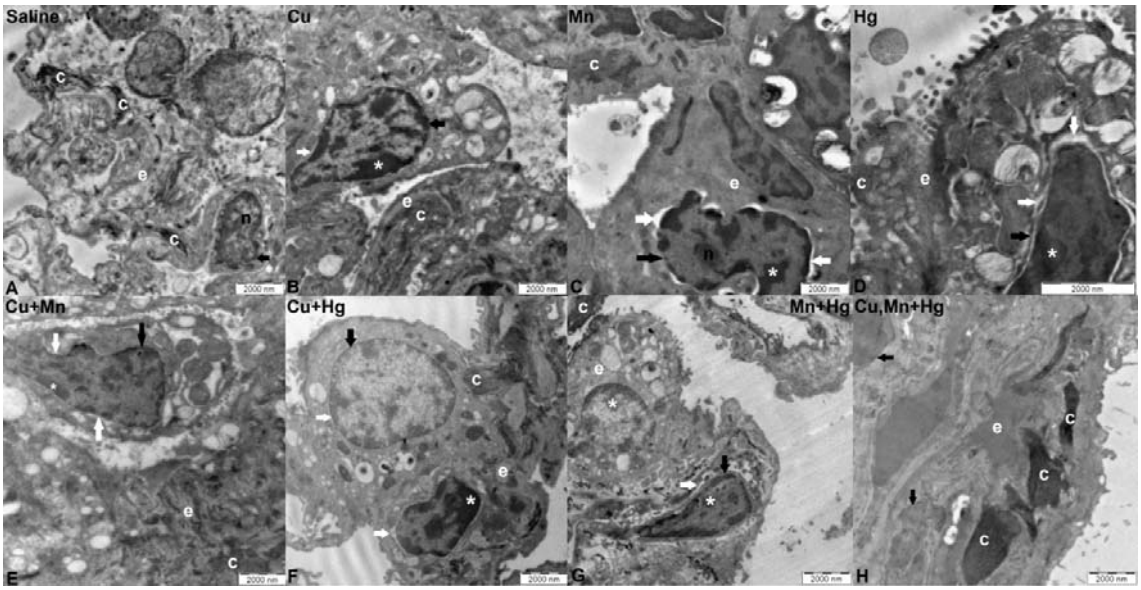

Figure 5: TEM micrographs of pulmonary tissue of SD rats exposed to Cu, Mn and Hg metal mixtures showing the ultrastructure of the tissue and demonstrating the nuclear membrane, nucleolus and arrangement of collagen and elastin fibres at a lower magnification; Scale bar = 2 µm. **A**: Control, **B**: Cu, **C**: Mn, **D**: Hg, **E**: Cu + Mn, **F**: Cu + Hg, **G**: Mn + Hg, and **H**: Cu, Mn + Hg. **Black arrows**: Nuclear membrane; **White arrows**: Nuclear membrane detachment; **c**: Collagen; **e**: Elastin; **n**: Nucleolus and **White asterisk**: Chromatin condensation.

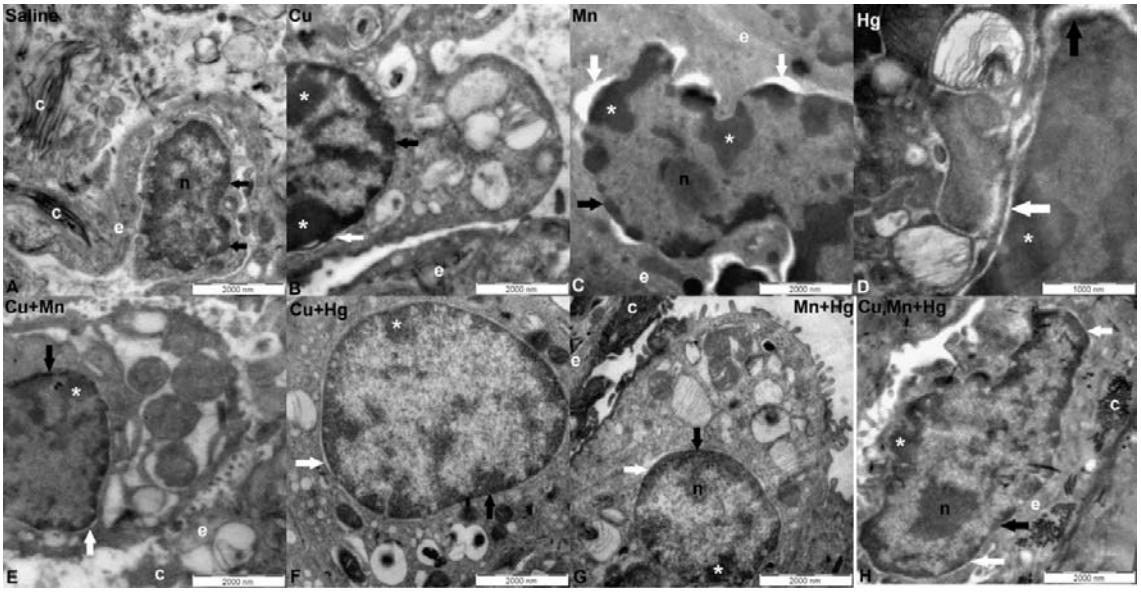

Figure 6: TEM micrographs of pulmonary tissue of SD rats exposed to Cu, Mn and Hg metal mixtures showing the ultrastructure of the tissue and demonstrating the nuclear membrane, nucleolus and arrangement of collagen

and elastin fibres at a higher magnification; Scale bar = 2 µm. **A**: Control, **B**: Cu, **C**: Mn, **D**: Hg, **E**: Cu + Mn, **F**: Cu + Hg, **G**: Mn + Hg, and **H**: Cu, Mn + Hg. **Black arrows**: Nuclear membrane; **White arrows**: Nuclear membrane detachment; **c**: Collagen; **e**: Elastin; **n**: Nucleolus and **White asterisk**: Chromatin condensation

Transmission electron microscopy

Representative pulmonary micrographs, acquired from control and exposed SD rat pulmonary tissue, with transmission electron microscopy, are shown in Figures 5 (low magnification) and 6 (high magnification). In Figures 5 A and 6 A, the ultrastructure of the control (saline) pulmonary tissue is shown and it demonstrates a typical type II pneumocyte with a central nucleolus (n) and a normal mixture of heterochromatin (electron dense areas) and euchromatin (electron-lucent areas) encased in the nuclear envelope (black arrows). The control group also demonstrated a few fine collagen (c) fibres. The pulmonary ultrastructure of the experimental groups are demonstrated in Figures 5 and 6 B - H. Overall, varying degrees of nuclear membrane detachment (white arrows), chromatin condensation (white asterisk), indistinct nucleoli and an increase in collagen fibre (c) bundles with disarrangement were demonstrated in all the experimental groups. It was also observed that the electron-lucent areas appeared less and the electron dense areas appeared greater in the experimental groups vs. the control. This is attributed to fewer elastin (e) fibres present in the control group.

A summary of the ultrastructural findings of the pulmonary tissues is presented in Table 3.

Table 3: Summary of the ultrastructural changes to pulmonary tissue following metal exposure.

	Indistinct nucleolus	Nuclear membrane detachment	Chromatin condensation	Increase in collagen fibres	Increase in elastin fibres
Cu	++	+	++	++	++
Mn	+	+++	++	+	++
Hg	++	++	++	+	+
Cu + Mn	++	+	+	+	++
Cu + Hg	++	+	++	++	++
Mn + Hg	+	++	+	++	++
Cu, Mn + Hg	+	+	++	+++	+++

–: no or minimal alterations; +: slight alteration; ++: moderate alteration; +++: severe alteration

Discussion

Air pollutants can cause severe lung injury and pathology, such as asthma and COPD. Bronchiole epithelium is the first line of defence against air particulate and pollutants. In the lungs the alveolar wall separates adjacent alveoli, which arise from the respiratory bronchioles [36, 37]. The alveolar wall consists of the lining alveolar epithelium, interstitium and the capillary of the endothelium forming the air-blood barrier for gaseous exchange.[37] The alveoli are stabilised and protected from over-distension and collapse by connective tissue and a surfactant layer, secreted by the type II pneumocytes. The inter-alveolar wall must provide stability, flexibility, and a large thin surface area for the effective diffusion of oxygen and carbon dioxide. [38]Although the effects of air pollution and associated heavy metals on the respiratory system are known, there is a lack of studies on the effect of orally exposed heavy metals on the respiratory system.

All the experimental groups demonstrated thickening of the inter-alveolar septa, a change to the intra-alveolar space area, desquamation of epithelia and a disruption of smooth muscle by connective tissue deposition and stratification/metaplasia of epithelium. Overall, Cu + Hg had the greatest toxic impact. In this group an extensive increase in yellow-red birefringence of collagen surrounding the bronchioles was observed, demonstrating an increase in collagen type I. Early fibrosis results in a high collagen type III to I ratio, whereas with late fibrosis this is in reverse.[39] Thus, early fibrosis was demonstrated in all experimental groups, while late fibrosis was observed for the Cu, Mn + Hg, Cu + Hg and the triple mixture groups (Figures 3.2 and 4.2). Similar changes were observed in rat lung tissue of SD rats exposed to Cd, Hg and the combined group at X1000 the WHO water limit. [3]

Proliferation and desquamation of alveolar epithelia can result in pulmonary fibrosis.[40] Desquamation of type II pneumocytes will affect the functionality and thus secretary properties of these cells.[41] Epithelial desquamation is a feature of acute severe asthma exacerbations and is associated with a decrease in the production of surfactant [41, 42]. Surfactant is essential in the prevention of alveolar collapse by decreasing the surface tension of the fluid that lines the alveoli. [42] A decrease in surfactant would therefore decrease the compliance of the lungs and increase inspiratory muscle effort to expand the lungs. [42] Other features demonstrated in asthma patients include qualitatively abnormal mucus, an increase in types I, III and V collagen, smooth muscle that undergoes hypertrophy and hyperplasia with an increase in the number and size of bronchiole blood vessels.[41] The collagen is deposited beneath the epithelium in asthma patients and this increases stiffness of the sub-epithelial matrix. [41] Epithelial disruptions can result in protein leakage from between the cells, which results in neutrophil recruitment and thus inflammation.[43] Inflammation will increase the volume of fluid in the lungs leading to a decreased rate of diffusion of gas according to Fick's law.[44]

Copper is used in industrial activities and the inhalation of it is associated with lung injury and pathology including fibrosis and epithelial apoptosis due to reactive oxygen species (ROS) production.[45] A dose of 200 mg/kg Cu ions causes a significant decrease in lung weight, in male SD rats.[46] A number of *in vivo* studies have demonstrated that copper oxide (CuO) nanoparticles are toxic to pulmonary tissue causing inflammation, which can lead to pulmonary fibrosis. [47-50] There are few studies on the toxic effects of Cu ions on pulmonary tissue, especially following oral exposure. Boyadzheiv *et al*., (2021) [51] investigated the toxic effects in murine pulmonary epithelium cells of Cu nanoparticle, microparticles and ions. At a concentration of 7 µg/mL copper chloride ($CuCl_2$) at 48-hrs incubation, multiple cellular pathways were affected and included oxidative stress, DNA damage and detoxification responses as well as cell cycle processes. Death-related transcripts, including five associated with autophagy and three associated with necrosis were also activated.[51] In a study by Camner *et al*., (1985) [52] the effect of inhaled Cu, among other metals, on rabbit lung tissue was investigated. Only slight inflammation was seen in the lung tissues exposed to aerosal Cu at concentrations of 1.1 and 3.9 mg/m^3 for 4-6 weeks and was associated with a significant increase in size of lung macrophages. No other weight or morphological changes were identified. [52]

In BALB/c mice exposed, via intraperitoneal injection, to 120 mg/kg Mn as methylcyclopentadienyl manganese tricarbonyl (MMT) the respiratory system was adversely affected.[53] These were features suggestive of diffuse interstitial pulmonary inflammation and degenerative changes to the bronchioles and alveolar ducts associated with interstitial thickening, hypercellularity and fibrosis. When subsequently exposed to an additional 80% oxygen, collagen accumulation and fibrosis were evident in the mice pulmonary tissues. After cessation of the exposure, lung tissue alterations were resolved after 3 weeks.[53]

Mercuric chloride ($HgCl_2$), at 5 mg/kg, increases alveolar wall thickness, induces alveolar collapse and haemorrhage and causes inflammatory cellular infiltration in male Kunming mice.[54] Wistar rats exposed to oral $HgCl_2$ 1.0 mg/kg per day had a significant increase in malondialdehyde (MDA), superoxide dismutase (SOD), catalase (CAT), glutathione peroxidase (GPx) and glutathione S-transferase (GST) compared with the control and other experimental groups treated with vitamin E and sodium selenite. Septal thickening, increase in inflammatory cells, fibrosis, oedema and haemorrhage were all evident in histopathological findings in the pulmonary tissue of the same group of rats.[55] Oral tissue directly exposed to $HgCl_2$ through dental amalgams, in rats (mothers and offspring), demonstrated vasodilation, infiltration of inflammatory cells, oedema, increase or degeneration of connective tissue and vacuolation dependant on time. [56] Occupational inhalation of Hg vapour can result in respiratory failure, emphysema of the mediastinum and muscle weakness.[57] A study by Lu *et al*., (2010) [58] showed various effects in the human lung invasive carcinoma cell line (Cl1-0) and mouse lung tissue after exposure to methylmercury chloride at 2.5–10 μM for 24–72 hrs and 0.2 mg/kg per day for 28 days, respectively. These effects included a decrease in cellular viability, an increase in MDA levels, an increase in ROS production, a decrease in surfactant protein messenger ribonucleic acid (mRNA) levels, and an increase in apoptotic markers and fibrosis. All the findings are indicative of mitochondrial cell death induced by oxidative stress in alveolar epithelial cells.[58]

Autophagy has become an important mechanism associated with pulmonary disease as it plays a role in pathogenesis but can also be a potential therapeutic target. The purpose of autophagy is to protect pulmonary cells by clearing molecules that can exacerbate inflammation, such as 168 oxidized proteins and phospholipids. However, the clearance of mitochondria may aggravate COPD by activating cellular death [59]. Infiltration and activation of inflammatory cells, such as neutrophils, can cause damage to pulmonary tissue due to prolonged granule

release and ROS production.[60] Trace heavy metals can be biomarkers of inflammatory lung disease. Elevated Mn levels have been found in asthma and bronchiectasis patients, while elevated Cu levels have been found in cystic fibrosis patients. [61]

In the current study, all the heavy metals caused nuclear detachment, condensation of chromatin and indistinct nucleoli of varying degrees were identified. These features are associated with pathological states and cell death signalling. The Mn group had the most nuclear detachment and thus the highest nuclear toxicity.

Elastin monomers are cross-linked through lysyl oxidase enzymes, which are Cu dependant. Abnormalities in pulmonary elastic fibre synthesis, deposition or degradation effects the normal functioning of the lung as elasticity is lost and there is a subsequent increase in alveolar space. This can result in COPD such as emphysema.[62] The volume fraction of the elastic fibres is reduced from 25.5% to 14.6% in the alveoli and the small airways of individuals with COPD as compared with normal individuals. [63]

Collagen is an important reinforcing fibre and alterations to it affect the mechanical properties of the tissues it reinforces.[64] Abnormal collagen orientation can result in pathological states. [64] Proper collagen orientation and density is important in preventing pulmonary changes such as thickening, which leads to narrowing and pulmonary dysfunction. These changes can occur through inflammation or injury. [64] Changes to collagen density, structure and quantity is seen in fibrotic pulmonary subepithelia.[64]

A field study on coppersmith's found 57% of the workers demonstrated abnormal pulmonary scans with lung disease patterns. Serum Cu levels were also significantly higher compared with the controls at 0.93 ± 0.14 mg/L.[65] Jiao *et al*., (2021) [66] reported that autophagy deficiency exacerbates acute lung injury caused by Cu oxide nanoparticles. The reduction in mitophagy

results in the accumulation of abnormal, non-functioning mitochondria that are overloaded with Cu ions. [66]

Pulmonary dysfunction occurs because of prolonged exposure to high concentrations of airborne Mn.[23] A cohort study done on the effect of Mn dust on exposed refinery workers found no effect in female workers, but a significant reduction in lung function in male workers exposed to high concentrations and in smokers vs. low concentrations and non-smokers, respectively.[67]

Tessier and Pascal (2006) [68], exposed human lung epithelial cells to 0.2 – 200 μM Mn, which caused a significant two to fourfold increase in intracellular phosphoproteins and subsequent release of inflammatory cytokines. An increase in intracellular phosphoproteins is an indicator of stress response, which includes the mediation of inflammation and the initiation of apoptosis. [68]

Acute Hg exposure can induce lung injury due to ROS overproduction and the depletion of antioxidants. Increased ROS plays a role in the regulation of cellular death and inflammation through inducing nuclear factor-κβ. [54] Acute exposure to high levels of elemental Hg vapour causes pulmonary distress and failure, bronchitis, pneumonia and pulmonary fibrosis (Smiechowics *et al.*, 2017).[69]

Besides the impact of oral exposure, few studies have been undertaken to investigate the effects of metal combinations. In a study, by Naidoo *et al.*, 2019 [3], adverse pulmonary effects were demonstrated in SD rats adminsitered the heavy metals Cadmium (Cd) and Hg at X1000 the WHO guidelines for drinking water. These effects included collapsed alveolar spaces, presence of inflammatory cells and thickening of the alveolar walls, increase in smooth muscle mass with luminal epithelium degeneration, detachment and aggregation within the bronchioles,

presence of prominent bronchiole-associated lymphoid tissue, fibrosis and dense collagen and prominent elastin arrangements.[3]

In general it appears that exposure to metal mixtures show increased pathogenesis due to inflammation, cellular damage and fibrosis and future research should focus on whether these effects are reversible and whether dietary antioxidant intervention can be beneficial.

Conclusion

In conclusion, all the heavy metal groups demonstrated toxic effects on pulmonary morphology and ultrastructure that will most likely alter physiological functioning. In all experimental groups, the metals had a negative impact on the pulmonary tissue with Cu + Hg and Mn causing the most severe and second most severe effects on pulmonary morphology, respectively. The Cu + Hg group demonstrated great yellow-red birefringence in the pulmonary tissue, indicating the development of late fibrosis. Fibrosis directly affects the physiological functioning of tissue and organs, while indirectly affecting organ systems and the functioning of the body leading to associated disease. Ultrastructurally, the pulmonary tissue had the highest sensitivity to the triple mixture group that caused the most alterations to elastin and collagen fibre bundles. Overall, Mn in any mixture caused deleterious effects with the Mn + Hg group showing the highest toxicity, which is probably mediated by increased ROS production that causes damage to membranes and the mitochondria.

References

1. Liu Q, Gao Y, Ci X. Role of Nrf2 and its activators in respiratory diseases. Oxid Med *Cell Longev*. 2019: 1–17. DOI:10.1155/2019/7090534.

2. Kim D, Chen Z, Zhou LF, Huang SX. Air pollutants and early origins of respiratory diseases. *Chronic Dis Transl Med*. 2018. 4(2): 75-94. DOI: 10.1016/j.cdtm.2018.03.003.
3. Naidoo SVK, Bester MJ, Arbi S, Venter C, Dhanraj P, Oberholzer HM. Oral exposure to cadmium and mercury alone and in combination causes damage to the lung tissue of SpragueDawley rats. *Environ Toxicol Pharmacol*. 2019. 69: 86-94. DOI: 10.1016/j.etap.2019.03.021.
4. Erhabor GE.. Respiratory health in Africa: Strides and challenges. *J Pan African Thoracic Soc*, 2021. 2(1): 11-17. DOI: 10.25259/JPATS_30_2020.
5. Kierszenbaum AL, Tres L, 2016. Histology and Cell biology: An Introduction to Pathology. 4th Ed. Elsevier Saunders.
6. Hamid Q; Tulic' MK, Liu MC, Moqbel R. Inflammatory cells in asthma: Mechanisms and implications for therapy. *J Allergy Clin Immunol*. 2003. 111(1): S5–S17. DOI:10.1067/mai.2003.22.
7. Karaman M, Arıkan Ayyıldız Z, Fırıncı F, Kiray M, Bağrıyanık A, Yilmaz O, Uzuner N, Karaman O. Effects of curcumin on lung histopathology and fungal burden in a mouse model of chronic asthma and oropharyngeal candidiasis. *Arch Med Res*. 2011. 42(2): 79-87. DOI: 10.1016/j.arcmed.2011.01.011.
8. Hamid, Q. Gross pathology and histopathology of asthma. *J Allergy Clin Immunol*. 2003. 111(2): 431–432. DOI:10.1067/mai.2003.147.
9. Molfino NA, Jeffery PK. Chronic obstructive pulmonary disease: Histopathology, inflammation and potential therapies. *Pulm Pharmacol Ther*. 2007. 20(5): 462–472. DOI:10.1016/j.pupt.2006.04.003.
10. Hogg J and Senior R. Chronic obstructive pulmonary disease c2: Pathology and biochemistry of emphysema. *Thorax*. 2002. 57(9): 830-834.

11. Suki B, Lutchen KR and Ingenito EP. On the progressive nature of emphysema: roles of proteases, inflammation, and mechanical forces. *Am J Respir Crit Care Med*. 2003. 168: 516-521.
12. Di Petta A. Histopathological characteristics of pulmonary emphysema in experimental model. *Einstein (Sao Paulo)* 2014. 12(3): 382-383. DOI: 10.1590/s1679-45082014ai2681.
13. Marcos JV, Muñoz-Barrutia A, Ortiz-de-Solórzano C, Cristóbal G. Quantitative assessment of emphysema severity in histological lung analysis. *Ann Biomed Eng*. 2015. 43(10): 2515-29. DOI: 10.1007/s10439-015-1251-5.
14. Mora AL, Torres-González E, Rojas M, Corredor C, Ritzenthaler J, Xu J, Roman J, Brigham K, Stecenko A. Activation of alveolar macrophages via the alternative pathway in herpesvirus-induced lung fibrosis. *Am J Respir Cell Mol Biol*. 2006. 35(4): 466-73. DOI: 10.1165/rcmb.2006-0121OC.
15. Raghu G, Weycker D, Edelsberg J, Bradford WZ, Oster Gerry. Incidence and prevalence of idiopathic pulmonary fibrosis. *Am J Respir Crit Care Med*. 2006. 174(7), 810–816.DOI:10.1164/rccm.200602-163OC.
16. King TE, Pardo A and Selman M. Idiopathic pulmonary fibrosis. *Lancet*. 2011. 378(9807): 1949- 1961.
17. Selman M, Pardo A. The epithelial/fibroblastic pathway in the pathogenesis of idiopathic pulmonary fibrosis. *Am J Respir Cell Mol Biol*. 2003. Sep;29(3 Suppl):S93-7.
18. Kim DS, Park JH, Park BK, Lee JS, Nicholson AG, Colby T. Acute exacerbation of idiopathic pulmonary fibrosis: frequency and clinical features. *Eur Respir J*. 2006. 27(1): 143-50. DOI: 10.1183/09031936.06.00114004. PMID: 16387947.

19. Fry DL, Hyatt RE. Pulmonary mechanics: A unified analysis of the relationship between pressure, volume and gasflow in the lungs of normal and diseased human subjects. *Am J Med*. 1960. 29: 672-689. DOI: 10.1016/0002-9343(60)90100-5.
20. Tsai N-C, Lee R-M. Interaction between cardiovascular system and respiration. *Appl Math Model*. 2011. 35(11): 5460–5469. DOI:10.1016/j.apm.2011.04.033.
21. Wildemann TM, Weber LP, Siciliano SD. Combined exposure to lead, inorganic mercury and methylmercury shows deviation from additivity for cardiovascular toxicity in rats. *J Applied Toxicol*. 2015. 35: 918-926.
22. Jaishankar M, Tseten T, Anbalagan N, Mathew BB, Beeregowda KN. Toxicity, mechanism and health effects of some heavy metals. *Interdisciplin Toxicol*. 2014. 7(2): 60-72.
23. Dorman DC, Struve MF, Gross EA, Wong BA, Howroyd PC. Sub-chronic inhalation of high concentrations of manganese sulfate induces lower airway pathology in rhesus monkeys. *Respir Res*. 2005. 6(1): 121-131.
24. Glezos JD, Albrecht JE, Gair RD. Pneumonitis after inhalation of mercury vapours. *Can Respir J*. 2006. 13(3): 150-152. DOI: 10.1155/2006/898120.
25. Oyarzún GMJ, Sánchez RSA, Dussaubat DN, Miller AME, González BS. Effect of copper sulphate on the lung damage induced by chronic intermittent exposure to ozone. *Revista Medica de Chile*. 2017. 145(1): 9-16.
26. Miller MA, Zachary JF. Mechanisms and morphology of cellular injury, adaptation, and death. *Pathol Basis Vet Dis*. 2017. 2-43.e19. DOI:10.1016/B978-0-323-35775-3.00001-1.
27. World Health Organization. Guidelines for drinking-water quality: fourth edition (2011). [Internet]. Available from:

https://www.unicef.org/cholera/Chapter_4_prevention/01_WHO_ Guidelines_for_drinking _water_quality.pdf.

28. Venter C, Oberholzer HM, Bester J, Van Rooy M-J, Bester MJ. Ultrastructural, confocal and viscoelastic characteristics of whole blood and plasma after exposure to cadmium and chromium alone and in combination: An ex vivo study. *Cell Physiol Biochem*. 2017. 43: 1288-1300.
29. van Rensburg MJ, van Rooy M-J, Bester MJ, Serem JC, Venter C, Oberholzer HM. Oxidative and haemostatic effects of copper, manganese and mercury, alone and in combination at physiologically relevant levels: An ex vivo study. *Hum Exp Toxicol.* 2019. 38, 419-433.
30. Arbi S, Bester MJ, Pretorius L, Oberholzer HM. Adverse cardiovascular effects of exposure to cadmium and mercury alone and in combination on the cardiac tissue and aorta of Sprague-Dawley rats. *J Environ Sci Health A Tox Hazard Subst Environ Eng*. 2021. 56(6): 609-624. DOI: 10.1080/10934529.2021. 1899534.
31. Nair AB, Jacob S. A simple practice guide for dose conversion between animals and human. *J Basic Clin Pharm*. 2016. 7(2): 27-31.
32. Latouff R, Younes R, Lutomski D, Naaman N, Godeau G, Senni K, Changotade S. Picrosirius red staining: a useful tool to appraise collagen networks in normal and pathological tissues. *J Histochem Cytochem*. 2014. 62(10): 751-758
33. Velindala S, Gaikwad P, Ella KKR, Bhorgonde KD, Hunsingi P, Anop K. Histochemical analysis of polarizing colours of collagen using Picro Sirius red staining in oral submucous fibrosis. *J Oral Health*. 2014. 6(1): 33-38.
34. Rigden HM, Alias A, Havelock T, O'Donnell R, Djukanovic R, Davies DE, Wilson SJ. Squamous metaplasia is increased in the bronchial epithelium of smokers with chronic

obstructive pulmonary disease. *PLoS One*. 2016. 11(5): 1-20. DOI: 10.1371/journal.pone.0156009.

35. Giroux V, Rustgi AK. Metaplasia: tissue injury adaptation and a precursor to the dysplasia-cancer sequence. *Nat Rev Cancer*. 2017. 17(10): 594-604. DOI: 10.1038/nrc.2017.68.
36. Robinson NE, Furlow PW. Anatomy of the respiratory system. *Equine Resp Med Surgery*. 2007. 1: 3-17.
37. Harkema JR, Nikula KJ, Haschek WM. Respiratory system. 3rd Ed. *Fundament Toxicol Pathol*. 2018. pg 351-393.
38. Knudsen L, Ochs M. The micromechanics of lung alveoli: structure and function of surfactant and tissue components. *Histochem Cell Biol*. 2018. 150(6): 661-676. DOI: 10.1007/s00418-018-1747-9.
39. Murtha LA, Schuliga MJ, Mabotuwana NS, Hardy SA, Waters DW, Burgess JK, Knight DA, Boyle AJ. The processes and mechanisms of cardiac and pulmonary fibrosis. *Front Physiol*. 2017. 8: 777-792. DOI: 10.3389/fphys.2017.00777
40. Farrell AP, MacLeod KR, Chancey B. Intrinsic mechanical properties of the perfused rainbow trout heart and the effects of catecholamines and extracellular calcium under control and acidotic conditions. *J Experiment Biol*. 1986. 125: 319-45.
41. Prescott G, Woodruff MPH, Bhakta NR, Fahy JV. Asthma: Pathogenesis and phenotypes. 6 th Ed. Murray and Nadel's Textbook of Respiratory Medicine. 2016. pgs 713-730.
42. Hohlfeld JM. The role of surfactant in asthma. *Resp Res*. 2002 3(1): 4-12. DOI: 10.1186/rr176.
43. Michaudel C, Mackowiak C, Maillet I, Fauconnier L, Akdis CA, Sokolowska M, Dreher A, Tan HT, Quesniaux VF, Ryffel B, Togbe D. Ozone exposure induces

respiratory barrier biphasic injury and inflammation controlled by IL-33. *J Allergy Clin Immunol*. 2018. 142(3): 942-958. DOI: 10.1016/j.jaci.2017.11.044.

44. Bateman RM, Sharpe MD, Ellis CG. Bench-to-bedside review: microvascular dysfunction in sepsis--hemodynamics, oxygen transport, and nitric oxide. *Crit Care*. 2003. 7(5): 359-373. DOI: 10.1186/cc2353.
45. Assad N, Sood A, Campen MJ, Zychowski KE. Metal-induced pulmonary fibrosis. *Curr Environment Health Rep*. 2018. 5(4): 486-498. DOI: 10.1007/s40572-018-0219-7.
46. Tang H, Xu M, Zhou XR, Zhang Y, Zhao L, Ye G, Shi F, Lv C, Li Y. Acute toxicity and biodistribution of different sized copper nano-particles in rats after oral administration. *Mat Sci Eng*. 2018. 93: 649-663. https://doi.org/10.1016/j.msec.2018.08.032.
47. Cho WS, Duffin R, Poland CA, Duschl A, Oostingh GJ, Macnee W, Bradley M, Megson IL, Donaldson K. Differential pro-inflammatory effects of metal oxide nanoparticles and their soluble ions in vitro and in vivo; zinc and copper nanoparticles, but not their ions, recruit eosinophils to the lungs. *Nanotoxicology*. 2012. 6(1):22-35. DOI: 10.3109/17435390.2011.552810.
48. Gosens I, Cassee FR, Zanella M, Manodori L, Brunelli A, Costa AL, Bokkers BG, de Jong WH, Brown D, Hristozov D, Stone V. Organ burden and pulmonary toxicity of nano-sized copper (II) oxide particles after short-term inhalation exposure. *Nanotoxicology*. 2016.10(8): 1084-95. DOI: 10.3109/17435390.2016.1172678.
49. Costa PM, Gosens I, Williams A, Farcal L, Pantano D, Brown DM, Stone V, Cassee FR, Halappanavar S, Fadeel B. Transcriptional profiling reveals gene expression changes associated with inflammation and cell proliferation following short-term

inhalation exposure to copper oxide nanoparticles. *J Appl Toxicol*. 2018. 38(3): 385-397. DOI: 10.1002/jat.3548.

50. Lai X, Zhao H, Zhang Y, Guo K, Xu Y, Chen S, Zhang J. Intranasal delivery of copper oxide nanoparticles induces pulmonary toxicity and fibrosis in C57BL/6 mice. *Scientific Reports*. 2018. 8(1): 4499-4527. DOI: 10.1038/s41598-018-22556-7.
51. Boyadzhiev A, Avramescu M, Wu D, Williams A, Rasmussen P, Halappanavar S. Impact of copper oxide particle dissolution on lung epithelial cell toxicity: response characterization using global transcriptional analysis. *Nanotoxicology*. 2021.15(3): 280-399.
52. Camner P, Curstedt T, Jarstrand C, Johannsson A, Robertson B, Wiernik A. Rabbit lung after inhalation of manganese chloride: a comparison with the effects of chlorides of nickel, cadmium, cobalt, and copper. *Environment Res*. 1985. 38(2): 301-309. DOI: 10.1016/0013- 9351(85)90094-5.
53. Hakkinen PJ, Morse CC, Martin FM, Dalbey WE, Haschek WM, Witschi HR. Potentiating effects of oxygen in lungs damaged by methylcyclopentadienyl manganese tricarbonyl, cadmium chloride, oleic acid, and antitumor drugs. *Toxicol Appl Pharmacol*. 1983. 67(1): 55-69. DOI: 10.1016/0041-008x(83)90244-2.
54. Liu B, Yu H, Baiyun R, Lu J, Li S, Bing Q, Zhang X, Zhang Z. Protective effects of dietary luteolin against mercuric chloride-induced lung injury in mice: Involvement of AKT/Nrf2 and NFκB pathways. *Food Chem Toxicol*. 2018. 113(2018): 296-302. https://doi.org/10.1016/ j.fct.2018.02.003.
55. Celikoglu E, Aslanturk A, Kalendar Y. Vitamin E and sodium selenite against mercuric chloride-induced lung toxicity in the rats. *Braz Arch Biol Technol*. 2015. 58(4): 587-594. DOI: 10.1590/S1516-8913201500098.

56. Soussa Essam, Shalaby Y, Maria A, Maria O. Evaluation of oral tissue response and blood levels of mercury released from dental amalgam in rats. *Arch Oral Biol*. 2013. 58(8): 981–988. DOI:10.1016/j.archoralbio.2013.03.012.

57. Smiechowicz J, Skoczynska A, Nieckula-Szwarc A, Kulpa K, Kübler A. Occupational mercury vapour poisoning with a respiratory failure, pneumomediastinum and severe quadriparesis. *SAGE Open Med Case Rep*. 2017. 5: 1-11. DOI: 10.1177/2050313X17695472.

58. Lu TH, Chen CH, Lee MJ, Ho TJ, Leung YM, Hung DZ, Yen CC, He TY, Chen YW. Methylmercury chloride induces alveolar type II epithelial cell damage through an oxidative stress-related mitochondrial cell death pathway. *Toxicol Lett*. 2010. 194(3): 70-78. DOI: 10.1016/j.toxlet.2010.02.003.

59. Ryter SW, Choi AM. Autophagy in lung disease pathogenesis and therapeutics. *Redox Biol*. 2015. 4: 215–225. https://doi.org/10.1016/j.redox.2014.12.010.

60. Grommes J, Soehnlein O. Contribution of neutrophils to acute lung injury. *Mol Med*. 2011. 17(3-4): 293-307. DOI: 10.2119/molmed.2010.00138.

61. Gray RD, Duncan A, Noble D, Imrie M, O'Reilly DS, Innes JA, Porteous DJ, Greening AP, Boyd AC. Sputum trace metals are biomarkers of inflammatory and suppurative lung disease. *Chest.* 2010. 137(3): 635-641. DOI: 10.1378/chest.09-1047.

62. Besiktepe N, Kayalar O, Ersen E, Oztay F. The copper dependent-lysyl oxidases contribute to the pathogenesis of pulmonary emphysema in chronic obstructive pulmonary disease patients. *J Trace Elements Med Biol*. 2017. 44: 247-255. DOI: 10.1016/j.jtemb.2017.08.011.

63. Black PN, Ching PST, Beaumont B, Ranasinghe S, Taylor G, Merrilees MJ.. Changes in elastic fibres in the small airways and alveoli in COPD. *Eur Resp J*. 2008 998- 1004. DOI: 10.1183/09031936.00017207.

64. Yang D, Yuan W, Lv C, Li N, Liu T, Wang L, Sun Y, Qiu X, Fu Q. Dihydroartemisinin supresses inflammation and fibrosis in bleomycin-induced pulmonary fibrosis in rats. *Int J Clin Exp Pathol.* 2015. 8(2): 1270-1281.

65. Dagli CE, Tanrikulu AC, Koksal N, Abakay A, Gelen ME, Demirpolat G, Yuksel M, Atilla N, Tolun FI. Interstitial lung disease in coppersmiths in high serum copper levels. *Biol Trace Element Res*. 2010. 137(1): 63-68. DOI: 10.1007/s12011-009-8566-8.

66. Jiao H, Jiang D, Hu X, Du W, Ji L, Yang Y, Li X, Sho T, Wang X, Li Y, Wu YT, Wei YH, Hu X, Yu L. Mitocytosis, a migrasome-mediated mitochondrial quality-control process. *Cell.* 2021. 184(11): 2896-2910. DOI: 10.1016/j.cell.2021.04.027.

67. Wang F, Zou Y, Shen Y, Zhong Y, Lv Y, Huang D, Chen K, Li Q, Qing L, Xia B, Su C, Ma S, Yang X. Synergistic impaired effect between smoking and manganese dust exposure on pulmonary ventilation function in Guangxi manganese-exposed workers healthy cohort (GXMEWHC). *PLoS One*. 2015. 10(2): 1-20. DOI: 10.1371/journal.pone.0116558.

68. Tessier DM, Pascal LE. Activation of MAP kinases by hexavalent chromium, manganese and nickel in human lung epithelial cells. *Toxicol Lett*. 2006. 167(2): 114-121. DOI: 10.1016/j.toxlet.2006.08.015.

69. Smiechowics J, Skoczynska A, Nieckula-Scwarc A, Kulpa K, Kubler A. Occupational mercury vapour poisoning with a respiratory failure, pneumomediastinum and severe quadriparesis. *Sage Open Med Case Rep*. 2017. 5 doi.org/10.1177/2050313X17695472